Journal of Power Technologies 105 (1) (2025) 77 -- 89

Improving PV system power using four-leg interleaved boost converter and MPPT based on robust integral linear quadratic control

MOHAMED CHERIF Daia Eddine Oussama ✉, CHEBABHI Ali, KESSAL Abdelhalim

Université Mohamed El Bachir El Ibrahimi de Bordj Bou Arréridj (Univ BBA), Bordj Bou Arreridj El-Anasser, 34030 , Algeria
✉ daiaeddineoussama.mohamedcherif@univ-bba.dz

Abstract

In this paper, a new robust integral linear quadratic controller (ILQC) is proposed for four leg interleaved boost converters (FLIBCs) used in the photovoltaic systems. Compared to classical boost converters (CBC), IBCs are used in the high power and voltage application. Therefore, the IBC can convert a high-current low-voltage input to a low-current high-voltage output and presents higher efficiency, lower current ripple, and better reliability. In order to enhance the photovoltaic system's robust performances as reliability and efficiency of the converter, the proposed robust ILQC is calculating with the consideration of equal current sharing. Results of the proposed technique are compared with those of a classical boost converter (CBC) and FLIBC based on PI control. Performances of FLIBC based on proposed ILQC are tested in several simulations using SimPower Systems and S-Function of MATLAB/SIMULINK. It is observed that the ILQC based FLIBC maximizes the conversion efficiency of photovoltaic systems, improving the response time, reducing the overshoot of the waveforms, and decreasing the current ripple. Compared to classical PI control, the proposed robust ILQC can increase the efficiency of conversion under different irradiance levels.

Keywords: Interleaved Boost Converter; Photovoltaic Systems; Integral Linear Quadratic Control; Maximum Power Point Tracking; Photovoltaic Efficiency

Introduction

In recent years, renewable energies have become a major research topic due to the high prices of traditional energies, and the emergence of myriad environmental problems such as pollution and global warming resulting from these traditional energies. In the last few years, photovoltaic system (PV) has become increasingly important as a green energy resource that is among the most widely used as a promising technology to replace the traditional energies [1]– [3].

DC/DC converter is one of the important parts that are used in photovoltaic systems to control the delivered power/voltage and to boost the photovoltaic output voltage into higher voltage level [4]. Several DC–DC converters topologies were proposed and used in the vast literature related to photovoltaic systems, one of the important power converters in use is the DC/DC boost converter, but it still is not able to give the demanded load power if the load voltage level is higher than the input voltage level [5].

To overcome the conventional boost converter problems, an interleaved boost converter (IBC) has

been proposed in [6]– [10]. IBC consists of parallel CBC connected to the same source and the same output. The feature of that topology is sharing the input current among the phases, reducing the input and output current ripple and the output voltage ripple [11]. The interleaved DC–DC boost converter is extensively utilized to boost the voltage into high voltage ratio, due to its advantages compared to DC/DC boost converter as a low current-ripple, high efficiency, better reliability and in particular, the IBC can convert a high-current low-voltage input to a low-current high-voltage output [9], [10], [12].

Technical challenges of the IBC are driving researchers to elaborate control strategies for IBCs based PV systems to improve their performances and to ensure maximum power point tracking of a photovoltaic system. In [12], a high voltage gains IBC with MPPT based on radial basis function network is compared with conventional MPPT based on P&O and fuzzy logic at different irradiation levels. In [13], output voltage control is proposed based on PI control for four phase IBC. Furthermore, Yin et Tun demonstrated the good performances given in the application of linear PI control for average input control of two-phase IBC [14]. Nevertheless, during the parameter variations and the coupled control channels of IBC, the manner of control presented isn't suitable for the PV systems and may lead to a lack of robustness to operating conditions. The PV system-based IBC shows highly nonlinear behavior making linear controllers not effective.

Researcher shows that several intelligent and advanced nonlinear controllers have been proposed and widely used for IBCs [15]–[17] to decouple the control channels, improving the dynamics of linear PI regulators increasing the robustness, the stabilization, giving good regulation on the dc voltage and the currents by the elimination of input and output current ripple and the output voltage ripple. Advanced nonlinear control plays an important part in the PV based on IBC.

To ensure maximum power point tracking of a PV system based on IBC, to regulate the output voltage, reduce the inductor current ripple, and also to ensure the sharing of total current carried between the different converter phases, El Fadil et al. [18] proposed a nonlinear adaptive sliding mode controller of a three-phase IBC to ensure asymptotical stability. However, the adaptive law is limited to external parameter variations. Thounthong et al. proposed a control law based on the differential flatness for IBC which given a solution to attain the maximum power point tracking without using a complicated algorithm [19]. In [20] a sliding mode controller was introduced to enhance the performance of the IBC to achieve the robustness and stability and taking into consideration the nonlinearity of the PV system based on IBC, this control is examined with classical PI controller to prove the high performance of the presented control. In [21] a robust control has been applied to an IBC using a hybrid strategy. Mohammad Rasool Mojallizadeh et al. proposed a switched linear control to improve the performance of the PV system based on IBC [22]. On the other hand, a simple linear quadratic controller (LQC) proposed in [23] compared with classical PI regulator in terms of robustness, references tracking under external parameter and loads variations, this technique offers a good high performance and is insensitive to external parameter and loads variations. Habib et all. [24] compared between the LQC based GA technique and the PI controller under undulation of current and load, as well as voltage variations. The LQC is a robust control technique that gives optimal control for linear systems with a given weighting matrices Q and R proposed in [23], [24]. Therefore, the dynamic performance of LQC used in the PV reference maximum power point tracking can deteriorate with some steady-state error introduced due to PV being subjected to variation with time [25].

To reduce this steady-state error and to increase the performance of a LQC, several other researchers have proposed a small modification of LQC by the introduction of integral action at the recently LQC. In [24], an LQR controller based on Genetic algorithms (GA) for two phases interleaved boost converter of fuel cell voltage regulation is proposed. In [25], a hybrid integral LQC (ILQC) is proposed for two-phase interleaved boost converter based microgrids under

power quality events which compared the performance between the ILQC technique and the classical LQC.

In this research work, a robust ILQC technique of the FLIBC based PV system is developed and proposed. The proposed technique is based on the integral action to reduce the steady-state error and to increase the performance in the two control loops of MPPT, which was used to the PV voltage control loop to maintain a constant DC voltage at the desired value and to generate the reference current of the current control loop. This in turn permitted good and permanent extraction of the maximum power from the PV system. The outputs of the current control loop are the duty cycles of FLIBC which shifted by (360/4) degree from each other. The performance of the proposed controller is proven by comparing its response with CBC and FLIBC based PI controller through simulation tests using Matlab/Simulink based SimPower Systems and S-Function, in order to evaluate the success, performance, robustness, effectiveness, and the ability of this technique to respond with minimal steady-state errors, lower voltage and current ripples under any external disturbance and parameter variations.

Mathematical modeling of FLIBC

The interleaved DC–DC boost converter is extensively utilized in PV sources to boost the voltage into high voltage ratio and to maximize the efficiency of conversion as shown in Fig. 1, due to its advantages as a low current-ripple, high efficiency, and in particular better reliability, the FLIBC can convert a high-current low-voltage input to a low-current high-voltage output. The schematic of FLIBC consists of four boost converters connected in parallel to the same PV system and output filtering capacitor. The switches have the same switching frequency and 90-degree phase shift. The inductor resistance is neglected. The resistor R is the load.

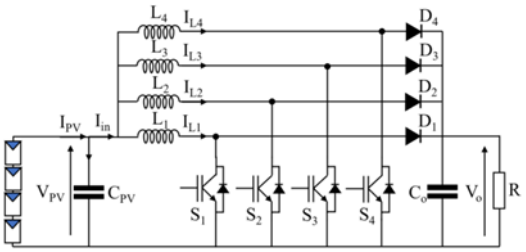

Figure 1: Four legs interleaved boost converter topology

Further, the differential equations that describe the appropriate dynamic model of the ICB topology are required to design the control. By evaluating the derivative of the four inductor currents and output capacitor voltage corresponding to the state of circuit when the switch S_j is ON, the following dynamic equations are given:

$$\begin{cases} L\dfrac{dI_j}{dt} = V_{PV} \quad ; j = 1,2,3,4 & (1) \\ C_{PV}\dfrac{dV_{PV}}{dt} = I_{PV} - I_{in} & (2) \end{cases}$$

When the switch S_j is OFF, the dynamic equations are given by:

$$\begin{cases} L\dfrac{dI_j}{dt} = V_{PV} - V_o \quad ; j = 1,2,3,4 & (3) \\ C_{PV}\dfrac{dV_{PV}}{dt} = I_{PV} - I_{in} & (4) \end{cases}$$

Where i_j is the inductor current, V_{pv}, and I_{pv} are PV system voltage and current respectively, I_{in} the FLIBC input current. $L=L_1=L_2=L_3=L_4$ input inductor and C_1 input capacitor.

By using the switch state $S_j \in \{0,1\}$, the differential equation describes the FLIBC dynamic performances as presented in (5) and (6):

$$\begin{cases} L\dfrac{dI_j}{dt} = V_{PV} - (1-S_j)V_o \quad ; j = 1,2,3,4 & (5) \\ C_{PV}\dfrac{dV_{PV}}{dt} = I_{PV} - I_{in} & (6) \end{cases}$$

The average model of PV system is used to get the state space form. By replacing the switch state S_j by its average value d_j during a sampling period ($<S_j>= d_j$). The differential equation describes the FLIBC dynamic performances as given by:

$$\begin{cases} L\dfrac{dI_j}{dt} = V_{PV} - (1-d_j)V_o \quad ; j = 1,2,3,4 & (7) \\ C_{PV}\dfrac{dV_{PV}}{dt} = I_{PV} - I_{in} & (8) \end{cases}$$

Control approach

Fig. 2 shows the control approach. It comprises two parts, the first part is the MPPT algorithm, and the other part is a dual loop control (two cascade PV current and voltage loops). The MPPT algorithm provides the PV system voltage reference to reach the maximum power point (MPP). The output of the voltage control loop acts as a reference value of current control loop to ensure the equal sharing of the current between the phases of FLIBC. The state feedback control strategy has been applied to allocate the poles of the closed-loop system. ILQC control allows calculating the state feedback gain by minimizing the performance index (PI) J. The optimization of PI is done by selecting two matrices Q and R, the weighting matrices for the state variable and the input variable, respectively. To design the ILQC controller, a state-space plant is required.

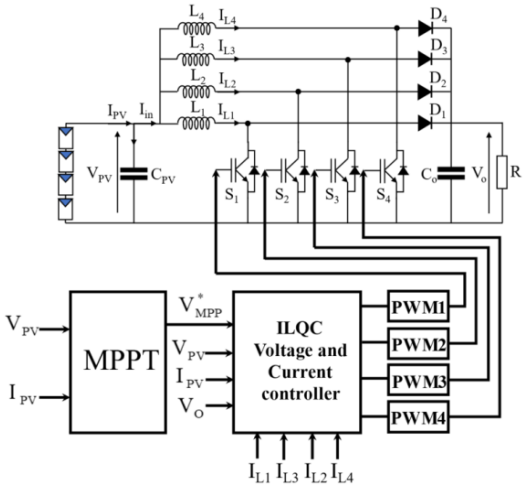

Figure 2: The control scheme of FLIBC based on ILQC technique

Consider a linear time-invariant system (LTI) given by its general form of state-space model:

$$\begin{cases} \dot{x}(t) = A\ x(t) + B\ u(t) \\ y(t) = C\ x(t) + D\ u(t) \end{cases} \quad (9)$$

Where x(t) is the state vector, u(t) is a control vector; A, B, C, and D are the state matrix, control matrix, output matrix, and feed-forward matrix, respectively. For the infinite horizon LQC problem, the time-invariant quadratic PI supposes the form:

$$J = \int_0^{\infty} (x^T(t)\ Q\ x(t) + u^T(t)\ R\ u(t))\ dt \quad (10)$$

Where Q is symmetric, positive semi definite matrix and R is symmetric, positive definite matrix.

In order to drive the PV system to their MPP and maximize the efficiency of conversion, the control that optimizes the PI is given by:

$$u(t) = -Kx(t) \quad (11)$$

And K presented as follow:

$$K = R^{-1}B^T P \quad (12)$$

Where P is the solution of algebraic Riccati equation (ARE), provided by the following equation:

$$A^T P + PA - PBR^{-1}B^T P + Q = 0 \quad (13)$$

Proposed ILQC-MPPT voltage and current controller loops

In order to extract the optimal and permanent maximum power from the PV system, an ILQC is developed for the two PV current and voltage loops to track the PV voltage to MPP voltage and keep it constant at the desired value by adjusting of FLIBC duty cycles. The first ILQC loop is proposed to ensure the PV voltage regulation and generate the inductance reference current for the second proposed current ILQC loop which ensures the PV current regulation to generate the FLIBC duty cycles with lower ripple in the voltage and current, and with minimal steady-state errors. ILQC-MPPT law depends on the PV voltage error; it represents the movement of the MPP operating point on the PV characteristics.

a) ILQC voltage control loop

Let us consider the state input and output vector as follows:

$$x=[V_{PV}] \quad u=[I_{PV}-I_{in}] \quad y=V_{PV} \quad (14)$$

From (8), (9), and (14) the outer loop system matrices are as follows:

$$A=0 \quad B=\frac{1}{C_{PV}} \quad C=1 \quad D=0 \quad (15)$$

To eliminate the steady-state error, an integral action is suggested. The new state space is given by the following presentation:

$$\dot{X}=\begin{bmatrix}\dot{x}\\ \dot{x}_i\end{bmatrix}=\begin{bmatrix}A & 0\\ -C & 0\end{bmatrix}\begin{bmatrix}x\\ x_i\end{bmatrix}+\begin{bmatrix}B\\ 0\end{bmatrix}u+\begin{bmatrix}0\\ 1\end{bmatrix}r \qquad y=\begin{bmatrix}C & 0\end{bmatrix}\begin{bmatrix}x\\ x_i\end{bmatrix} \quad (16)$$

So, the new matrices become as follows:

$$A=\begin{bmatrix}0 & 0\\ -1 & 0\end{bmatrix} \quad B=\begin{bmatrix}\frac{1}{C_{PV}}\\ 0\end{bmatrix} \quad C=\begin{bmatrix}1 & 0\end{bmatrix} \quad D=0 \quad (17)$$

Where:

$$K=\begin{bmatrix}K_v & K_i\end{bmatrix} \quad (18)$$

b) ILQC Current control loop

To design the current controller, a state space is required where the state vector, input, and output vector are considered as:

$$x=[i_j] \quad u=[V_{PV}-(1-d_j)V_o] \quad y=i_j \quad (19)$$

From (7), (9) and (19) the inner loop matrices are defined as:

$$A=0 \quad B=\frac{1}{L_j} \quad C=1 \quad D=0 \quad (20)$$

Scale the reference with gain N will scale the output to the desired level.

$$N=(C(BK-A)^{-1}B)^{-1} \quad (21)$$

The duty cycle d_j that will be delivered to the PWM block is derived from the control vector of the inner loop where:

$$d_j=1+\frac{u_j-V_{PV}}{V_o} \quad (22)$$

Fig. 3. shows a block diagram of proposed ILQC-MPPT voltage and current controller loops.

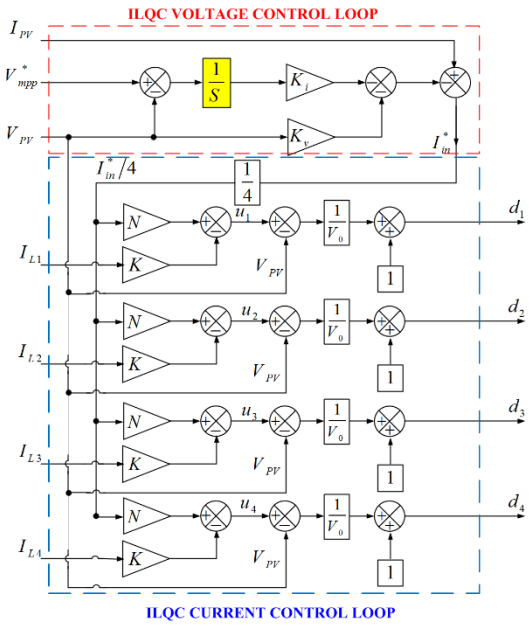

Figure 3: Block diagram of proposed ILQC-MPPT voltage and current controller loops

Results and discussion

In order to validate the proposed ILQC technique, a four-phase interleaved DC-DC boost converter-based PV system simulation model has been developed using SimPower System and S-Function of MATLAB/Simulink. Block diagram of the control schemes are shown in Fig. 2. The system has been simulated under varying irradiation and the temperature has been maintained constant (25º C) as shown in Fig. 4. The subjects of these simulations are the study of following aspects: (a) The PV system output current, the converters input current, and the improvement of PV system output power quality for FLIBC rating in comparison with CBC controlled by conventional PI due to four phases IBC controlled by conventional PI and proposed ILQC. (b) The effects of proposed ILQC for the response time and overshoot, the current ripple, the error between the PV power and their MPP reference, compensation of four-phase interleaved DC–DC boost converter currents, PV system output current and converter input current under changing irradiation. The system and controllers' simulation parameters are presented in Table 1 and Table 2 respectively. Performance comparison of the all-converter topology and their controllers (CBC based PI controller, FLIBC based PI controller, and FLIBC based ILQC) is given in the figures (Figs. 4–9).

Table 1: The Simulink model parameter values

System	Parameter	Value
PV system	V_{co}	21.83 V
	V_{mpp}	17.27 V
	I_{sc}	5.33 A
	I_{mpp}	4.93 A
	P_{max}	4x85.15 W
FLIBC	C_{PV}	63 uF
	C_o	3.2 uF
	L1=L2=L3=L4	8 mH
	R	320
	f_s	50 KHz

Table 2: The PI and ILQC parameter values

System	PI	ILQC
Voltage control loop	K_p= 0.2	Q= $\begin{bmatrix} 0.01 & 0 \\ 0 & 2800 \end{bmatrix}$
	K_i= 161.28	R= 0.1
Current control loop	K_p= 50.27	Q= 342
	K_i= 78977	R= 0.0171

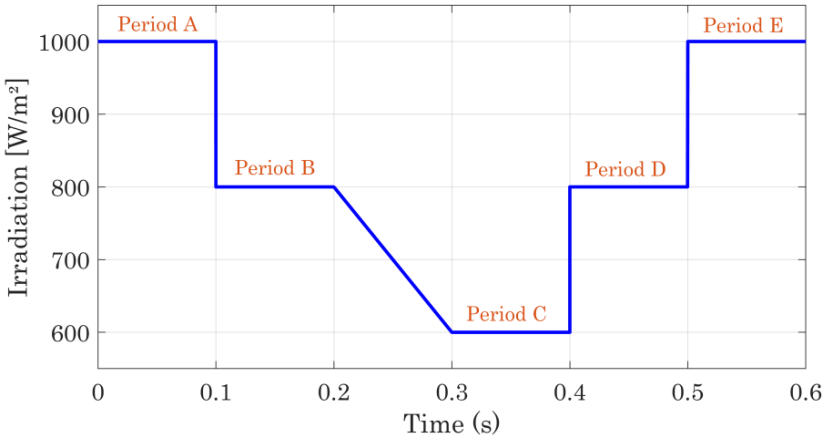

Figure 4: The solar irradiation used in the simulation

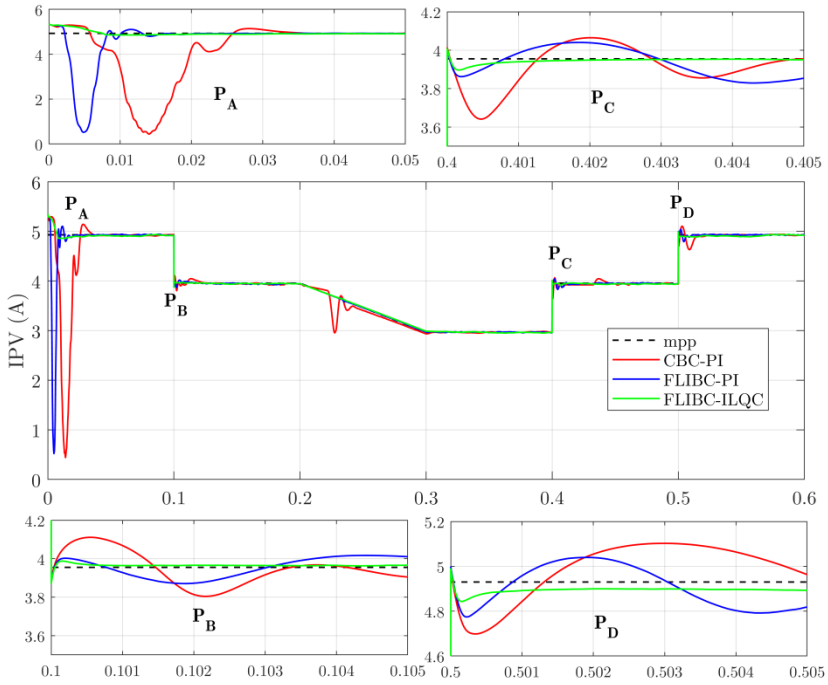

Figure 5: PV system output current for all-converters topology and control (CBC based PI controller, FLIBC based PI controller, and FLIBC based ILQC)

Fig. 5 illustrated the PV system output current behaviors under irradiation varying from 600 to 1000 W/Km2 and IpvMPP reference current varying from 3 to 5 A and inversely in the all-converter topologies and controllers. The comparison of these behaviors shows that the PV system output current track perfectly the IpvMPP reference current with zero steady state error in the all-converter topologies and controllers. It can be observed that the overshoot and ripple in the all points (A,B,C and D) and periods (A,B,C and D) (zoom

of all points) are greatly reduced with very small response time in the case of ILQC based FLIBC compared to other converter topologies and controllers, as shown in the four zoom of Fig. 7. It is also clearly observed in all points and periods that the ILQC rejects all perturbation at the variation of irradiance. The comparative study of overshoot, ripple and response time based on the simulation results of the all-converter topology and their controllers has been achieved and presented in Table 3.

The input current of all converters and four inductors currents are shown in Fig. 6, 7 and 8 respectively. The comparison of the input current of all converters under varying irradiance in terms of ripple, steady state error, overshoot, and response time is shown in Figs. (6 and 7). It is observed that ILQC based FLIBC has enhanced its performance more than the other converter topologies and controllers as it has less rise time, much better response time, zero overshoot and steady state, and more robustness under all perturbation at the variation of irradiance. This comparison is detailed in Table III. Similarly, Fig. 8 shows the four inductors currents behaviors for the FLIBC based on ILQC and PI, respectively. It is observed that the four inductors currents are equal and a very low ripple is shown in both ILQC based FLIBC and PI based FLIBC, and each inductor current is equal to one-fourth of the FLIBC input current in all points and periods under all varying irradiance. It is therefore confirmed that the FLIBC is capable to ensure the equal current sharing between four inductors.

The behaviors of PV system output power in the all - converter topologies and controllers are shown in Fig. 9. Based on these behaviors, it is observed that the disturbances of the irradiation changes are rejected in the all-converter topologies and controllers, and the behaviors increase the power conversion efficiency of the FLIBC topology compared to the CBC topology as shown in the four zoom of Fig. 9. It is also clearly observed in all points and periods that the ILQC based FLIBC converges to MPP with very small response time and zero overshoot and zero steady state error compared to PI based CBC and PI based FLIBC under all perturbation at the variation of irradiance, which confirms the effectiveness and the good dynamic performances of the PV system based on FLIBC controlled by ILQC in terms of power and current quality.

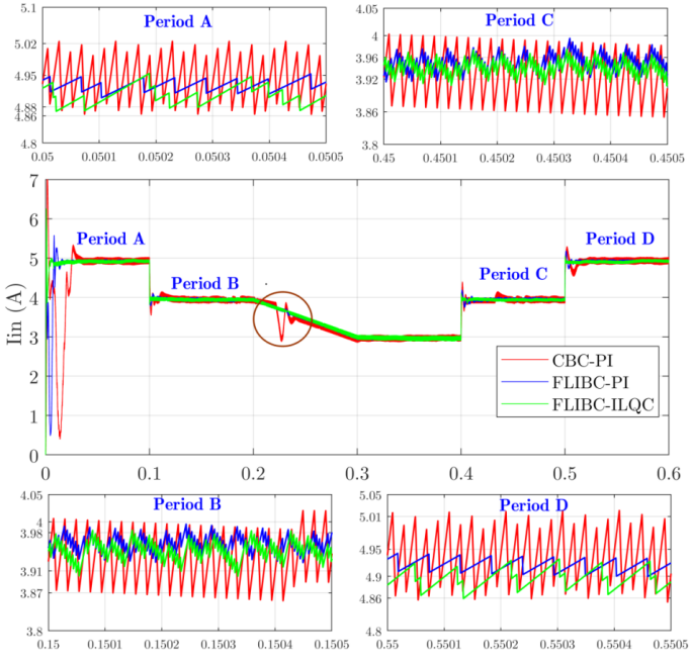

Figure 6: Input current ripple for all-converter topology and controllers

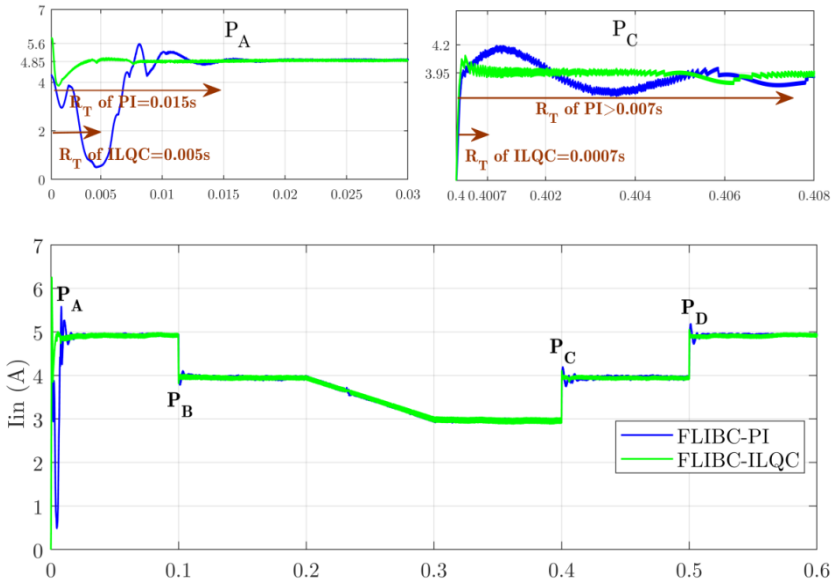

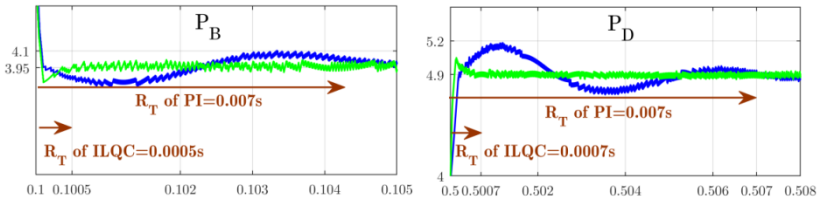

Figure 7: Input current response time and overshoot for all-converter topology and controllers

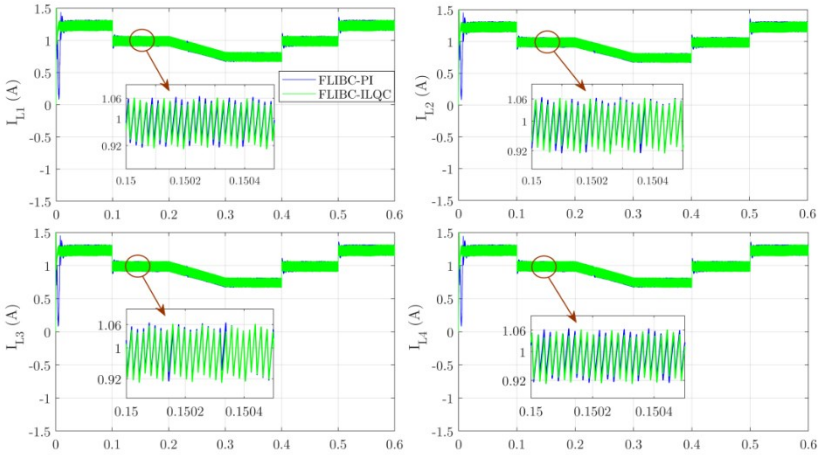

Figure 8: Four legs interleaved boost converter inductors currents

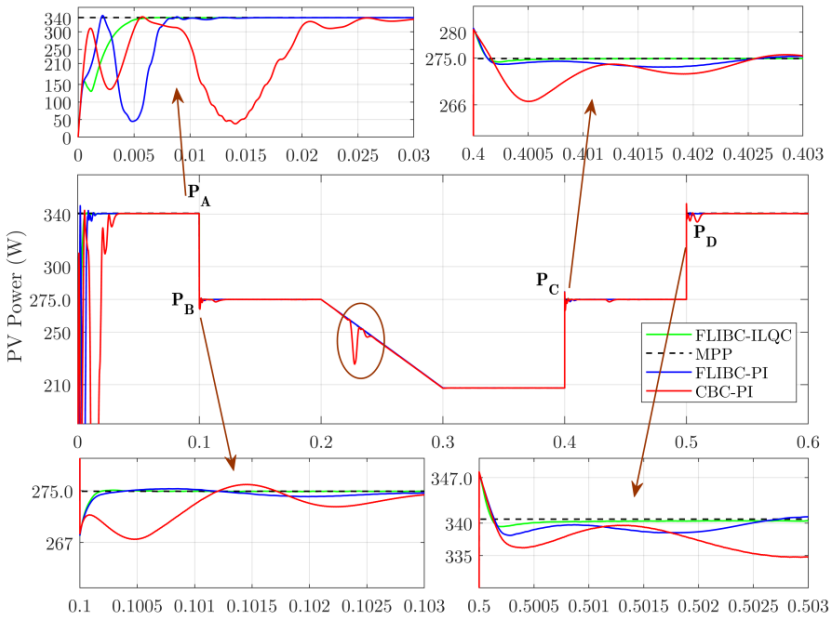

Figure 9: PV system output power for all-converter topology and controllers

Table 3 shows a comparison between the ripple value in the input current, output current, inductors current and output voltage in each converter scheme. The comparison shows that the ripple value is reduced with the FLIBC topology and the ILQC control shows superiority compared to the PI controller in this point of view.

Table 3: The ripple of the input current, output current, and the output voltage in each case

	CBC with PI	FLIBC with PI	FLIBC with ILQC
I_{in}(A)	0.1760	0.0703	0.0682
I_o(A)	0.0022	0.0004	0.0003
I_L(A)		0.1611	0.1594
V_o(V)	1.3740	0.1110	0.1050

Conclusion

In this paper an interleaved DC-DC boost converter connected to a PV system based ILQC is proposed. The proposed scheme allows controlling the PV system voltage and assuring extracting the maximum power and the equal sharing of input current between each phase of FLIBC.

The results of ILQC are compared with the results of CBC and FLIBC based PI which show that the proposed ILQC is more satisfactory and improves the performance of the system. Therefore, the FLIBC based ILQC is suitable to use for enhancing the conversion efficiency in photovoltaic applications.

In this research work, a FLIBC based on ILQC technique has been developed and proposed for the PV system application. The proposed technique is based on the integral action to reduce the steady-state error and to increase the performance in the two control loops, which are used to the PV voltage control loop to maintain a constant DC voltage at the desired value and to generate the reference current of the current control loop permitting a good extraction and permanent value of the maximum power from the PV system. FLIBC is proposed to reduce all current ripples, sharing the FLIBC input current equally between the four leg inductors, and to reduce the power switches problems, thus enhancing the efficiency of the FLIBC. To validate the performance and the effectiveness of the proposed FLIBC based on ILQC it has been compared with CBC based on PI and FLIBC based on PI through simulation tests using Matlab/Simulink based SimPower Systems and S-Function under varying irradiance. The simulation comparative standard performance and robustness results for all-converter topologies and controllers demonstrate that the proposed FLIBC based on ILQC performed better than the CBC based on PI and FLIBC based on PI.

The proposed FLIBC based on ILQC can be used in PV system for several power applications such as renewable energy sources, electric vehicles, motor drives, battery chargers, and power quality enhancement in grids, which gives good dynamic performance as response time and lower current ripple, as well as in PV system output power and voltage. The advantages of using FLIBC for maximum power point extraction from PV system are the good dynamic response time and very lower ripple.

Acknowledgements

This work is supported by DGRSDT Algeria, with collaboration of LPMRN Laboratory at Bordj Bou Arreridj University, and GE Laboratory of M'sila

References

1. S. Gallardo-Saavedra and B. Karlsson, "Simulation, validation and analysis of shading effects on a PV system," Sol. Energy, vol. 170, no. May, pp. 828–839, 2018, doi: 10.1016/j.solener.2018.06.035.

2. G. Ciulla, V. Lo Brano, V. Di Dio, and G. Cipriani, “A comparison of different one-diode models for the representation of I-V characteristic of a PV cell,” Renew. Sustain. Energy Rev., vol. 32, pp. 684–696, 2014, doi: 10.1016/j.rser.2014.01.027.
3. M. A. Elgendy, B. Zahawi, and D. J. Atkinson, “Evaluation of perturb and observe MPPT algorithm implementation techniques,” IET Conf. Publ., vol. 2012, no. 592 CP, 2012, doi: 10.1049/cp.2012.0156.
4. ZEBIRI, Fouad et al. Analysis and Design of Photovoltaic Pumping System based on Nonlinear Speed Controller. Journal of Power Technologies, [S.l.], v. 96, n. 1, p. 40--48, apr. 2016. ISSN 2083-4195.
5. K. S. Tey and S. Mekhilef, “Modified incremental conductance MPPT algorithm to mitigate inaccurate responses under fast-changing solar irradiation level,” Sol. Energy, vol. 101, pp. 333–342, 2014, doi: 10.1016/j.solener.2014.01.003.
6. A. S. Samosir, N. Taufiq, and A. H. Mohd Yatim, “Simulation and Implementation of Interleaved Boost DC-DC Converter for Fuel Cell Application,” Int. J. Power Electron. Drive Syst., vol. 1, no. 2, pp. 168–174, Oct. 2011, doi: 10.11591/ijpeds.v1i2.126.
7. C. Chen, C. Wang, and F. Hong, “Research of an interleaved boost converter with four interleaved boost convert cells,” in 2009 Asia Pacific Conference on Postgraduate Research in Microelectronics & Electronics (PrimeAsia), Nov. 2009, pp. 396–399, doi: 10.1109/PRIMEASIA.2009.5397361.
8. T. Xue, Z. Minxin, and Y. Songtao, “Maximum power point tracking for photovoltaic power based on the improved interleaved boost converter,” in 2016 IEEE 11th Conference on Industrial Electronics and Applications (ICIEA), Jun. 2016, no. 1, pp. 2215–2218, doi: 10.1109/ICIEA.2016.7603957.
9. A. S. Samosir, M. Anwari, and A. H. M. Yatim, “Dynamic evolution control of interleaved boost dc-dc converter for Fuel Cell application,” in 2010 Conference Proceedings IPEC, Oct. 2010, pp. 869–874, doi: 10.1109/IPECON.2010.5697088.
10. S. Z. Mirbagheri, S. Mekhilef, and S. M. Mirhassani, “MPPT with Inc . Cond method using conventional interleaved boost converter,” Energy Procedia, vol. 42, pp. 24–32, 2013, doi: 10.1016/j.egypro.2013.11.002.
11. N. Rana, M. Kumar, A. Ghosh, and S. Banerjee, “A Novel Interleaved Tri-State Boost Converter With Lower Ripple and Improved Dynamic Response,” IEEE Trans. Ind. Electron., vol. 65, no. 7, pp. 5456–5465, Jul. 2018, doi: 10.1109/TIE.2017.2774775.
12. J. REDDY and S. NATARAJAN, “Control and Analysis of MPPT Techniques for Standalone PV System with High Voltage Gain Interleaved Boost Converter,” Gazi Univ. J. Sci., vol. 31, no. 2, pp. 515–530, 2018.
13. I. Laoprom, S. Tunyasrirut, W. Permpoonsinsup, and D. Puangdownreong, “Voltage Control with PI Controller for Four Phase Interleaved Boost Converter,” in 2019 16th International Conference on Electrical Engineering/Electronics, Computer, Telecommunications and Information Technology (ECTI-CON), Jul. 2019, pp. 278–281, doi: 10.1109/ECTI-CON47248.2019.8955211.
14. Y. Y. Phyo and T. L. Naing, “Implementation the Average Input Current Mode Control of Two-Phase Interleaved Boost Converter,” vol. 12, no. 10, pp. 770–780, 2018, doi: 10.5281/zenodo.1474982.
15. G. M. Vargas-Gil, J. C. Colque, A. J. Sguarezi, and R. M. Monaro, “Sliding Mode plus PI Control applied in PV Systems Control,” 2017 6th Int. Conf. Renew. Energy Res. Appl. ICRERA 2017, vol. 2017-January, pp. 562–567, 2017, doi: 10.1109/DISTRA.2017.8191124.
16. A. Dali, S. Abdelmalek, and M. Bettayeb, “A Backstepping Controller for Interleaved Boost DC–DC Converter Improving Fuel Cell Voltage Regulation,” 2021, pp. 751–762.
17. R. B. A. Cunha, R. S. Inomoto, J. A. T. Altuna, F. F. Costa, S. G. Di Santo, and A. J. Sguarezi Filho, “Constant switching frequency finite control set model predictive control applied to the boost converter of a photovoltaic system,” Sol. Energy, vol. 189, no. June, pp. 57–66, 2019, doi: 10.1016/j.solener.2019.07.021.

18. H. El Fadil, F. Giri, and J. M. Guerrero, “Adaptive sliding mode control of interleaved parallel boost converter for fuel cell energy generation system,” Math. Comput. Simul., vol. 91, pp. 193–210, May 2013, doi: 10.1016/j.matcom.2012.07.011.
19. P. Thounthong, S. Pierfederici, and B. Davat, “Analysis of Differential Flatness-Based Control for a Fuel Cell Hybrid Power Source,” IEEE Trans. Energy Convers., vol. 25, no. 3, pp. 909–920, Sep. 2010, doi: 10.1109/TEC.2010.2053037.
20. A. H. Kardile, A. Z. Khuzani, and S. M. Mule, “Sliding Mode Control Based 2Nx Interleaved Boost Converter for Solar PV Applications,” in 2018 Second International Conference on Intelligent Computing and Control Systems (ICICCS), Jun. 2018, pp. 1273–1278, doi: 10.1109/ICCONS.2018.8663166.
21. R. Saadi, M. Y. Hammoudi, O. Kraa, M. Y. Ayad, and M. Bahri, “A robust control of a 4-leg floating interleaved boost converter for fuel cell electric vehicle application,” Math. Comput. Simul., vol. 167, pp. 32–47, Jan. 2020, doi: 10.1016/j.matcom.2019.09.014.
22. M. R. Mojallizadeh and M. A. Badamchizadeh, “Switched linear control of interleaved boost converters,” Int. J. Electr. Power Energy Syst., vol. 109, no. June 2018, pp. 526–534, 2019, doi: 10.1016/j.ijepes.2019.02.030.
23. M. Habib and F. Khoucha, “An Improved LQR-based Controller for PEMFC Interleaved DC-DC Converter,” Balk. J. Electr. Comput. Eng., vol. 3, no. 1, pp. 30–30, Feb. 2015, doi: 10.17694/bajece.46410.
24. M. Habib, F. Khoucha, and A. Harrag, “GA-based robust LQR controller for interleaved boost DC – DC converter improving fuel cell voltage regulation,” Electr. Power Syst. Res., vol. 152, pp. 438–456, 2017, doi: 10.1016/j.epsr.2017.08.004.
25. G. H. Valencia-Rivera, I. Amaya, J. M. Cruz-Duarte, J. C. Ortíz-Bayliss, and J. G. Avina-Cervantes, “Hybrid Controller Based on LQR Applied to Interleaved Boost Converter and Microgrids under Power Quality Events,” Energies, vol. 14, no. 21, p. 6909, Oct. 2021, doi: 10.3390/en14216909.